ARTICLES

Synchrotron Light Scattering on Nanostructured V/Ce Oxide Films Intercalated with Li^+ Ions†

P. Dubček,‡ A. Turković,*,‡ Z. Crnjak Orel,§ B. Etlinger,‡ and S. Bernstdorff||

Institute "Ruđer Bošković", P.O. Box 180, HR-10002 Zagreb, Croatia, National Institute of Chemistry, Hajdrihova 19, SI 1001 Ljubljana, Slovenia, and Sincrotrone Trieste S.c.p.A., ss. 14, km 163,5 Basovizza, 34012 Trieste, Italy

Received October 29, 2003

Vanadium oxide and new V/Ce oxide films on a glass substrate were obtained by the sol−gel process. The morphology of these nanostructured and porous films was studied by grazing-incidence small-angle X-ray scattering (GISAXS) at the ELETTRA synchrotron (Italy, Trieste). The aim of performing GISAXS was to study changes, which might occur in the grain sizes and the porosity of vanadium oxide and V/Ce oxide at 38 and 55 atom % of V, upon the intercalation of Li^+ ions. The average grain radius $\langle R \rangle$ obtained by GISAXS varied with the layer thickness and upon the intercalation of Li^+ ions. The layer structure in V/Ce oxides was revealed by the grazing-incidence X-ray reflectivity (GIXR) method. The average grain radius $\langle R \rangle$, obtained by GISAXS, was correlated with the intercalation of Li^+ ions. The specific surface area of these films was also determined and generally varied from 0.5 nm^{-1} to 0.03 nm^{-1}.

1. INTRODUCTION

The past few decades have been marked by the study of new materials on the mesoscopic scale (2−50 nm), such as deposited layers, multilayers, and more recently clusters, aggregates, and nanosized materials. Nanostructured materials are hierarchically structured on different length scales down to the atomic or the grain size level. Investigation of such a structure requires new experimental techniques to understand the structure at all levels of organization. In this context, new techniques have been developed to obtain accurate measurements of the structure on an atomic scale and medium range scale.

In the above-mentioned period a great interest was shown in the preparation of nanostructured oxides using the sol−gel process. The most important thing in the sol−gel procedure is the preparation of a sol that presents a stabile colloidal suspension. Later films or coating can be prepared from sols on a substrate by the dip coating technique. By this procedure pure and mixed oxide systems were easily prepared. In our previous papers on Ti, Ce, Ce/Sn, V, and V/Ce oxides obtained by the sol−gel procedure a grazing-incidence small-angle X-ray scattering (GISAXS) was presented.[1−15] This method allows for the morphological characterization of nanostructured materials. Besides it, an adequate, nondestructive, and highly versatile method for a complete characterization of interfaces in multilayer structures is the grazing-incidence X-ray reflectivity (GIXR).

The grazing-incidence X-ray reflectivity can provide detailed information about the thickness of single layer, multilayer periodicity, and thickness of the individual layers that make up a multilayer. GIXR information also includes determination of root-mean square (rms) roughness on internal interfaces and on the external surface.

The full potential of these techniques is realized when using a synchrotron source (flux, collimation, and choice of wavelength to avoid fluorescence or to perform anomalous measurements) and when patterns are recorded with two-dimensional detectors.

Measurements were performed using synchrotron radiation at ELETTRA, Trieste, which has a thousand times higher intensity than a laboratory X-ray tube. The results of these measurements are presented in this work.

2. EXPERIMENTAL SECTION

Vanadium oxide and V/Ce oxide films on a glass substrate were prepared by the sol−gel dip-coating method, which are presented in previous publications.[1−15]

GISAXS and GIXR measurements were performed at a new SAXS beamline at synchrotron ELETTRA, Trieste.[16,17] The beamline is built by the researchers from the Institute for Biophysics and X-ray Structure Research (IBR), Austrian Academy of Science. Its characteristics are as follows: the photon beam wavelength is $\lambda = 0.154$ nm, the energy resolution is $\Delta E/E \leq 2.5 \times 10^{-3}$, the focal spot size fwhm is 1.2×0.6 mm^2, the spot at the sample is 5.4×1.8 mm^2, the flux at the sample is 5×10^{12} photons, and the angular divergence of a beam is 1 mrad horizontal and 0.3 mrad vertical (electron beam energy 2 GeV, beam current 200 mA, X-ray photon energy 8 keV). The shape and size of the incident beam was controlled by Huber slits ($h = 0.1$ mm,

† This paper is published in honor of the former Editor-in-Chief of JCICS Dr. George W. A. Milne.

* Corresponding author phone: ++385-1-4561-086; fax: ++385-1-4680-114; e-mail: turkovic@rudjer.irb.hr.

‡ Institute "Ruđer Bošković".

§ National Institute of Chemistry.

|| Sincrotrone Trieste S.c.p.A.

10.1021/ci030419j CCC: $27.50
Published on Web 02/12/2004

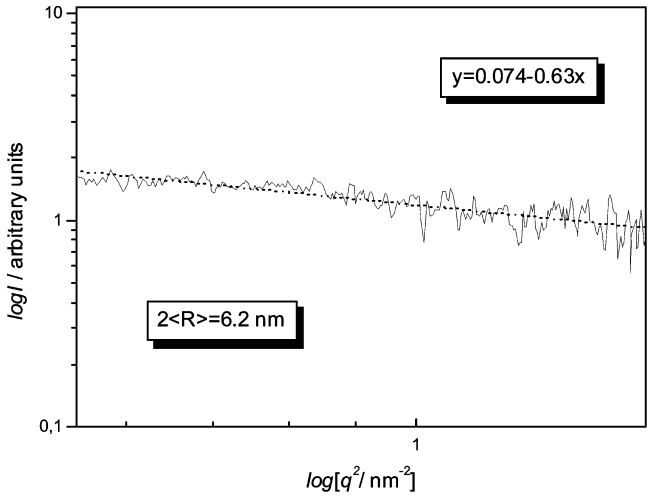

Figure 1. Linear fit to $\log(I) = f(q)$ for GISAXS data on sample with V_2O_5 oxide intercalated with Li^+ ions.

$w = 5$ mm). The sample was mounted on a stepper-motor-controlled tilting stage with a step resolution of 10^{-3}°.

Grazing-incidence X-ray reflectivity (GIXR) is the experimental technique that combines both grazing incidence and reflectivity. In this geometry the path of X-rays through the thin film is much longer than for standard transmission geometry, and the substrate signal is weak. In this geometry the totally reflected power is superimposed on the scattering signal at higher values of $q = 4\pi\theta/\lambda$.[18] In our experiments the grazing angle has been changed in the range 0.1°, −1.1° approximately, and the steps varied from 0.01° to 0.1°.

3. RESULTS

Thin V_2O_5 and mixed oxides films on the glass substrate can be considered as aggregates containing nanoparticles or nanograins and pores.[9,10,14,15] In this case, the SAXS is caused by the difference of electron density within and around the nanoparticles. Using the Guinier approximation[19] (the scattering in the very small angle range is of Gaussian form, independent of the shape of the present particles) the sizes can be readily determined. Porod approximation[20−22] is suitable to determine the specific surface area of nanostructured thin films. In our previous measurements[23] with an ordinary X-ray source the intensity of a recorded signal was too small to get the part of a curve relevant for Porod approximation. With high intensity of synchrotron light sources the scattered intensity is high enough that we can apply both approximations and obtain both relevant parameters, i.e., grain sizes and specific surfaces of V_2O_5 and mixed oxides thin films. In this section the outline of calculations in the Guinier and Porod approximations is given for V/Ce oxide with 38 atom % of V intercalated with Li^+ ions, but it was successfully applied for all other oxides as TiO_2, CeO_2, V_2O_5, and mixed Ce/Sn and V/Ce oxides.

Figure 1 represents the data for V_2O_5 intercalated with Li^+ ions in a $\log(I)$ vs $f(q^2)$, $q = 4\pi\theta/\lambda$, plot as a test as to whether one can apply the above-mentioned Guinier law: $I(q) = (\Delta\rho)^2\exp(-Rg^2q^2/3)$ for a small q. The "average particle radii" can be estimated from the radius of gyration, Rg, in the Guinier formula. They were calculated from the slopes in the linear fit of $\log(I)$ vs $f(q^2)$ (nm^{-2}) for an annealing temperature of 673 K. From these fitting lines we have obtained Rg and an average particle radius R using $R = (5/3)^{1/2}$ Rg (for spherical shape).

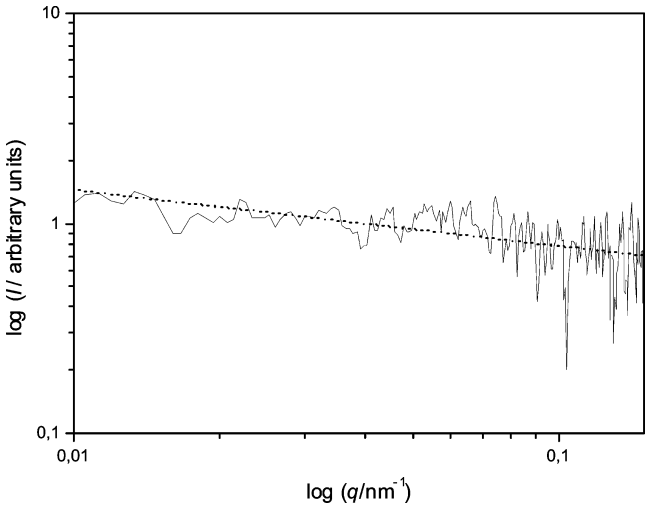

Figure 2. Representation of the data as $\log(I) = f[\log(q)]$ as a test for applying the general Porod formula.

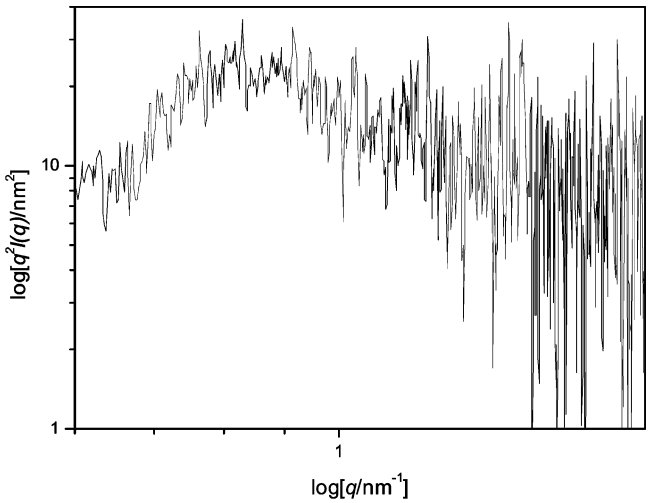

Figure 3. Plot of integral value of intensity multiplied by q^2 in the q space. The obtained value for S_s is equal to 141.5 nm^{-1} for V_2O_5 oxide intercalated with Li^+ ions.

The fitting line in Figure 2 with a slope of −4 indicates that the Porod law, $I(q) = 2\pi(\Delta\rho)^2S/q^4$, can be applied for V_2O_5 with Li^+ at a larger q. GISAXS results for both, pure and intercalated V_2O_5, agree with the AFM photographs of these samples.[25] Taking that into account the "specific surface area", S_s, can be calculated from the Mittelbach-Porod formula[20−22]

$$S/V = \pi\{\lim_{q\to\infty}[q^4I(q)]\}/Q \qquad (1)$$

where Q is the invariant integral

$$\int_0^\infty q^2I(q)dq$$

which we have approximated by the value Q_{max}:

$$Q_{max} \equiv \int_{min}^{max} q^2I(q)dq$$

shown in Figure 3 where $q_{max} = 1.8$ nm^{-1}.

Figure 4 represents the data in the $q^4I(q)$ vs q plot for the high values of q. For $q \geq 0.9$ nm^{-1} the constant value of q^4I

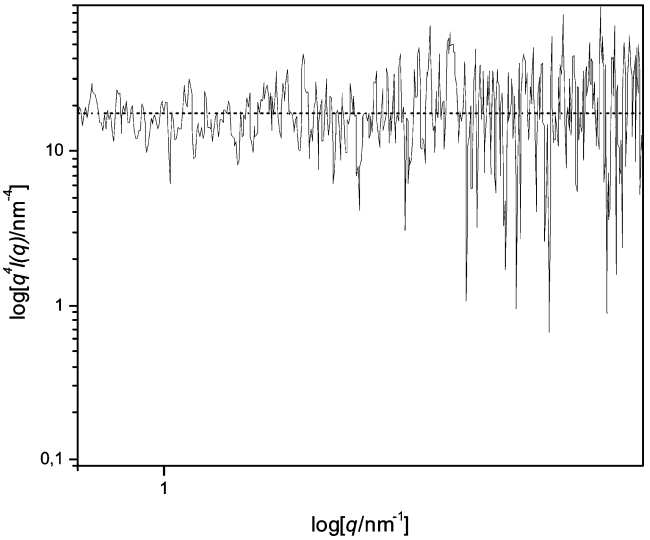

Figure 4. Plot of $q^4I(q)$ vs q as a limes to higher values of q. The value of $2\pi\rho^2S$ from our graph is equal to 4.7 nm^{-4}.

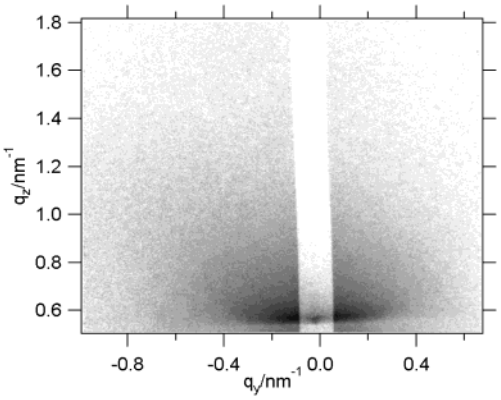

Figure 5. 2-D intensity pattern of GISAXS for V_2O_5 oxide. The brighter vertical strip is caused by an attenuator used to deplete the strong specular signal.

$= 2\pi\rho^2S$ is used to calculate the specific surface area from formula 1 for the V_2O_5 film.

The presence of the grains is best illustrated by Figure 5, where a two-dimensional scattered intensity pattern from the sample V_2O_5 is shown, as taken with the two-dimensional CCD detector. The whiter vertical strip at $q_y = 0$ is the area of lowered intensity depleted by an attenuator. This is the specular plain position, where the surface scattering is present, and its intensity is typically much higher than the particle scattering from within the film. The 1D detector scattering data have been taken in the specular plane.

The diffuse intensity left and right from the specular plane is isotropic SAXS scattering due to the porous and particulate structure of the film. Because of the random distribution of the particles and the pores throughout the film, the scattered intensity does not depend on the surface orientation, and therefore it is distributed evenly in all directions for the given angle between the scattered and the direct beam direction.

In the case of a highly rough surface, combined with a high electron density contrast in the sample, the diffuse scattering can have the intensity higher than the respective surface scattering, as is shown in Figure 6, where the specular and the off specular scattering are compared, taken for $q_y = 0$ and $q_y = 0.1$ nm^{-1}, respectively, with the intensities renormalized to the same high angle level. Apart from the minor difference close to the critical angle i.e., the Yoneda peak position, the two intensities are virtually equal. Obviously, the isotropic scattering is dominant also in the specular plane.

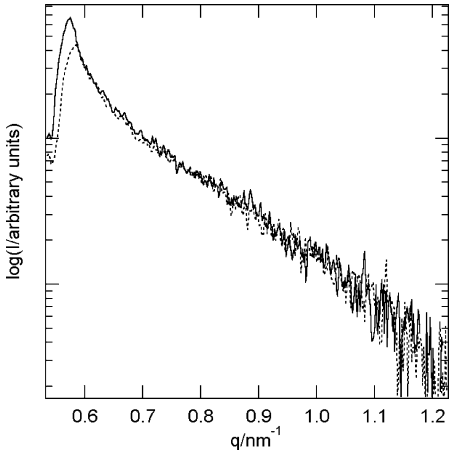

Figure 6. Specular (full line) and off specular (dashed line) intensity vs scattering wave vector q_z taken from 2 D data shown in Figure 4a for $q_y = 0$ and $q_y = 0.1$ nm^{-1}, respectively. The intensities have been renormalized to the same tail value.

4. DISCUSSION

4.1. GISAXS in V_2O_5 and $V_2O_5-CeO_2$ Thin Films on the Glass Substrate. Vanadium oxide, such as V_2O_5, has been extensively studied because it tends to form a layered structure that allows the intercalation/deintercalation of different ions between its layers. It can be used as a catalyst, in an electrochromic device, in an advanced electrochemical cell concept, especially in lithium batteries.[24] Our previous measurements of morphology of this material have shown its nanosized beside layered structure.[25,26] To make a complete characterization of interfaces in a layered structure of vanadium and V/Ce oxide films on glass substrates, we have performed grazing-incidence X-ray reflectivity (GIXR).[10] We have compared the GIXR characterization of layers with GISAXS grain sizes and specific surfaces of V_2O_5 and V_2O_5 /CeO_2 oxides and obtained insight into the grain size distribution within the layer.

The grain size is determined for V/Ce oxides for sets of fixed grazing angles. They were changed in the range from 0.3° to 1.1° with a step of 0.1° and repeatedly with smaller steps of 0.01°, 0.02°, and 0.05°. The average grain sizes calculated from the Guinier equation for all samples are shown in Table 1. Supported by AFM photographs[25] the "specific surface area", S_s, was calculated from the Mittelbach-Porod formula (1) and as well shown in Table 1.

Our analysis of measurements at the synchrotron light source was done by a graphical method of calculation for the grain size and the specific surface, which determines porosity. The average radius of mixed oxides shows a difference for the values of pure V_2O_5. For the sample of V/Ce oxide at 38 atom % V at a grazing angle of 0.5°, as presented in Table 1, the specific surface S_s is equal to 0.190 nm^{-1}, which is smaller than a 0.304 nm^{-1} value for pure V_2O_5.[10] Pure V_2O_5 for a grazing angle at 0.5° has bigger grains $\langle D\rangle = (10.78 \pm 2.54)$ nm and higher porosity than a mixed V/Ce oxide at 38 atom % V with $\langle D\rangle = (6.86 \pm 2.56)$ nm. Pure V_2O_5 for all grazing angles has higher porosity

Table 1. V_2O_5/CeO_2 Samples, Annealing Temperature, Grazing Angle, "Average Grain Radius" $\langle R \rangle$ and "Specific Surface Area" S_s as Determined from GISAXS

sample	annealing T (K)	grazing angle (°)	GISAXS $\langle R \rangle$ (nm)	GISAXS S_s (nm^{-1})
V_2O_5	673	0.3	6.73 ± 1.38	0.198
V_2O_5	673	0.5	5.39 ± 1.27	0.304
V_2O_5	673	0.7	3.51 ± 1.37	0.674
V_2O_5	673	0.9	2.94 ± 0.74	1.574
V_2O_5	673	1.0	2.26 ± 0.92	2.030
55%	673	0.3	5.10 ± 1.42	0.083
55%	673	0.5	4.24 ± 1.19	0.168
55%	673	0.7	2.43 ± 0.79	0.244
55%	673	0.9	2.09 ± 0.76	0.472
55%	673	1.0	2.15 ± 0.54	0.550
38%	673	0.3	8.43 ± 2.20	0.120
38%	673	0.5	3.43 ± 1.28	0.190
38%	673	0.7	1.93 ± 0.94	0.500
38%	673	0.9	1.45 ± 0.59	1.150
38%	673	1.0	1.86 ± 0.51	1.720

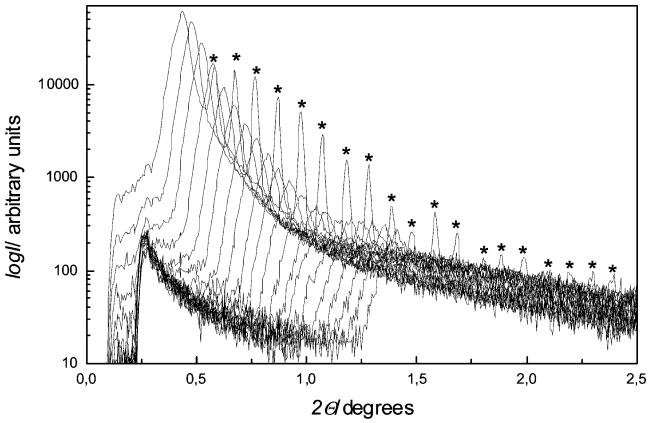

Figure 7. Reflectivity at grazing angles from 0.3° to 1.25° with a fixed step of 0.05° for 38 atom % V in V/Ce oxide.

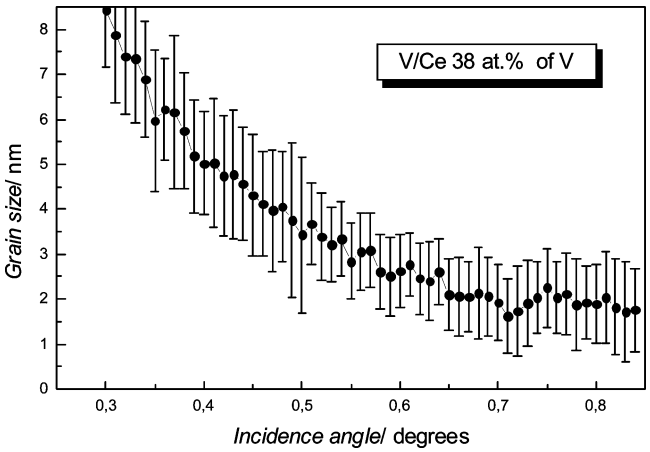

Figure 8. Average grain sizes as a function of grazing angles in 38 atom % V in V/Ce oxide.

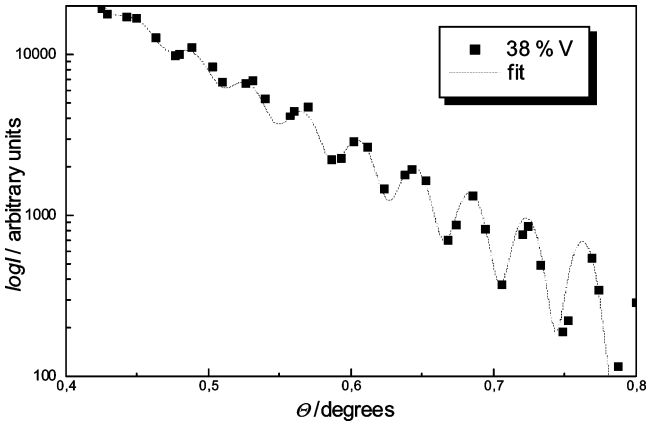

Figure 9. Reflectivity envelope for 38 atom % V in V/Ce oxide.

than mixed V/Ce oxides at 38 atom % and 55 atom % V. Grain size determined by XRD[26] is in accordance with our results. All values for $\langle R \rangle$ and S_s are in agreement within the errors limits with the results from previous work.[10] Addition of cerium dioxide to vanadium pentoxide increased the stability of vanadium pentoxide during 700 cycles of charge−discharge with a constant current. V/Ce oxide is an intercalation electrode in an electrochemical cell with lithium electrolyte ($LiClO_4$ in propylene carbonate). Mixed V/Ce oxide with 38 atom % V shows the biggest capacity for the intercalation of Li ions in comparison with other V/Ce oxides and is equal to 300 C/m.[225]

Figure 7 shows a two-dimensional plot of GISAXS curves in a sequence of fixed grazing angles for V/Ce oxide with 38 atom % V. Simultaneously to the GIXR data, from these measurements we have obtained grain sizes and specific surfaces for each step of the grazing angle. After the critical angle of 0.366° for our films, X-ray starts to penetrate into the bulk of the film. Grazing angles are connected with the penetration depth of X-rays in the film.

Figure 8 shows a grain size distribution with the grazing angles of V/Ce oxide with 38% of atomic percent of V. The average grain size $\langle R \rangle \sim 8$ nm at 0.3° and decreases to $\langle R \rangle \sim 2$ nm at 0.8°. After 0.6° the grain size is almost constant and averages 2 nm. The specific surface has an opposite trend, and at 0.6° it shows a considerable rise from 0.24 nm^{-1} to 1.15 nm^{-1} at 0.8°.

From the calculated penetration depth, the depth size distribution of grains and specific surfaces were obtained in our previous work.[10] There are plots showing comparison of S_s and $\langle R \rangle$ values obtained by Guinier and Porod approximations for various penetration depths of X-rays in the film.[10]

4.2. GIXR in V_2O_5 and $V_2O_5-CeO_2$ Thin Films on the Glass Substrate. The GIXR data were taken with a Gabriel type, gas filled 1D detector in a sequence of fixed grazing angles. Figure 7 shows a two-dimensional plot of GISAXS curves in a sequence of fixed grazing angles. From this sequence of detector scans, X-ray reflectivity data are extracted. Integral intensities of these specular peaks, denoted with a star (*), were extracted, with the diffuse intensity subtracted and plotted versus the scattering angle Θ at which they appear. The thus obtained grazing-incidence X-ray reflectivity data are shown in Figure 9 as the reflectivity peak's envelope for V/Ce oxide with 38 atom % V. It reveals a continuous disorder of a single layer of V/Ce oxide with 38 atom % V,[9,10,25,26] which occurs due to the roughness of the SnO_2:F covered glass substrate and local fluctuations of the layer thickness. The distance between successive minima is connected to the thickness of the layer through a law similar to the Bragg law, but a more complex theoretical model is given by the distorted wave Born approximation (DWBA).[27]

Table 2. V_2O_5/CeO_2 and the Same Ones Intercalated with Li^+ Ions Samples, Grazing Angle, "Average Grain Radius" $\langle R \rangle$ as Determined from GISAXS, Surface Roughness from AFM, "Specific Surface Area" S_s as Determined from GISAXS

sample 673 K	grazing angle (°)	GISAXS $\langle R \rangle$ (nm)	AFM s.r. (nm)	GISAXS S_s (nm^{-1})	GISAXS Li $\langle R \rangle$ (nm)	AFM s.r. (nm)	GISAXS Li S_s (nm^{-1})
V_2O_5	0.5	5.39 ± 1.27	11	0.304	3.10 ± 0.58	6	1.130
55%	0.5	4.24 ± 1.19	40	0.168	4.37 ± 0.72	30	0.040
38%	0.5	3.43 ± 1.28	2	0.192	4.90 ± 0.43	8	0.033

The index of refraction for X-ray propagation in solids is slightly less than 1, i.e., $n = 1 - \eta' - i\eta''$, where $\eta'$and η'' are the dispersion and absorption coefficients, respectively. Their typical values are $\eta' \sim 10^{-6}$ and $\eta'' \sim 10^{-8}$. Therefore, the total reflection happens for angles smaller than $\alpha_C = \sqrt{(2\eta')}$. For wider angles and for small surface roughness ($q_z^2\sigma^2 \ll 1$, where q_z is the scattering wavevector and σ is the surface roughness), reflectivity is given by DWBA as

$$|r|^2 = |r_F|^2 \exp[-q_z\, q_z^{\,t}\, \sigma^2] \quad (2)$$

where q_z^t is the scattering wavevector in the solid and r_F is the Fresnel reflectivity, which, in the approximation of small grazing angles, is given by

$$r_F = (q_z - q_z^{\,t})/(q_z + q_z^{\,t}) \quad (3)$$

In the presence of a thin film of a different index of refraction than the substrate, both interfaces are contributing; therefore, the specular reflectivity can be written as[28]

$$R_{tot} = \{r_2 + r_3 \exp[2ik_0\theta_2 d]\}/\{1 + r_2 r_3 \exp[2ik_0\theta_2 d]\} \quad (4)$$

where d is the film thickness, k_0 is the wave vector in a vacuum, and

$$r_j = \{[\theta_{j-1} - \theta_j]/[\theta_{j-1} + \theta_j]\} \exp[-2k_0^{\,2}\theta_{j-1}\theta_j\sigma_j^{\,2}] \quad (5)$$

is the Fresnel reflectivity on the border between the two media. r_2 and r_3 designate air/film and film/substrate interface reflectivity, θ_j is the beam angle in the film ($j = 2$) and in the substrate ($j = 3$), and σ_j is the interface roughness. The angle θ is an approximation of sin θ.

From the reflectivity peak's envelope for V/Ce oxide prepared at 38 atom % of V the film thickness is $d = (217.2 \pm 0.1)$ nm. A spread of the upper surface is equal to $\sigma_{up} = 2.9$ nm and that of the lower surface in contact with the substrate is $\sigma_{down} = 0.1$ nm.

The thickness of amorphous V/Ce films on the SnO_2:F substrate obtained by a theoretical fit is determined with precision to angstroms. The obtained values for a layer thickness are $d = (107.9 \pm 0.1)$ nm and $d = (218.8 \pm 0.1)$ nm for V_2O_5 and V/Ce oxide prepared at 55 atom % of V, respectively. The surface roughness of the external surface is determined with 10% precision, but the spread of contact surface with the substrate is in the range of 0.1−0.5 nm.

The results obtained with the GIXR and GISAXS analyses of the data are complementary to build a model of the layers and their grain size structure. The grain size distribution by GISAXS at different grazing angles i.e., different depths of the film reveal a possible existence of an inner-layered structure in the film. Transmission electron microscopy measurements (TEM)[29] verified our results obtained with the GIXR experiment.[10] TEM photographs will be published in a paper by Crnjak Orel et al.[29]

4.3. GISAXS in V_2O_5 and $V_2O_5-CeO_2$ Thin Films Intercalated by Li^+ Ions on the Glass Substrate. We prepared CeO_2/SnO_2[4,5,30,31,32] and mixed V/Ce oxide[9,10,14,15,25,26] films via an inorganic sol−gel route as a counter electrode for a smart window. Our aim was to prepare a stable counter electrode deposited by only one dipping. Samples at different atomic ratios of V/Ce (78, 55, 38, and 32 atom % of V in V/Ce oxide) were prepared on a K-glass. The best capacity (~300 C/m^2 for one dip layer) for the intercalation/deintercalation of Li^+ in 1 M $LiClO_4$ in propylene carbonate (PC) was obtained for samples at 55 and 38 atom % of V. Not only that the capacity of prepared films was improved but also the electrochemical stability in a wide range (+2 to −1.5 V vs Ag/AgCl) of pureV_2O_5 films was much improved after the addition of CeO_2. The best samples which can serve as a counter electrode were obtained at 55 and 38 atom % of V in V/Ce oxide.[25,30] Pure V-oxide and these two samples as thin films and powder were characterized by IR spectroscopy.[25,30] The samples in a powder form were also analyzed by Raman spectroscopy. The obtained results show the formation of crystalline V_2O_5 in the samples prepared without the addition of CeO_2. The formation of V_2O_5 and $CeVO_4$ was found in a mixed sample prepared at 55 atom % of V in V/Ce oxide. Additionally, we established the formation of an amorphous phase at 38 atom % of V, which contained the tetrahedral species of VO_4^{3-}.

The addition of cerium improved the stability of vanadium oxide with the ion-charge capacity (up to 300 Cm^{-2}). The intercalation of Li^+ ions in V/Ce films was followed by FT-IR spectroscopy in combination with CV measurements at a wide potential range and now by GISAXS measurements as shown in Table 2. It contains data for the grazing angle at 0.5°, as the critical angle for V_2O_5 equals 0.366°. That means that the X-ray penetrates a sample at angles bigger than 0.366°. As we have previously seen AFM photographs[25] showing surface change upon the intercalation of Li^+ ions, we are here interested in changes inside the bulk of the film, that results in grazing angles > 0.4°.

Table 2 contains grain sizes and porosity for vanadium pentoxide and two mixed oxides with 55 and 38 of atom % of V prior and after the intercalation of Li^+ ions. It can be observed that grain sizes are decreasing with the increase of CeO_2 in mixed oxides. Porosity decreases after the intercalation of Li ions in mixed oxides, which is in agreement with the picture of Li^+ ions filling empty space in a porous electrode upon the intercalation process. After the intercalation of Li^+ ions grain sizes decrease in the case of V_2O_5 but increase for V/Ce oxide with 38 atom % of V.

The case of V/Ce oxide with 55 of atom % of V is special, as it has a fractal dimension of $D_f = 3.75$ nm obtained from the coefficient of direction in the $\log(I) = f[\log(q)]$ plot. For volume fractals in a regime of polydispersity $\tau > 2$, the

fractal dimension is obtained from the equation[33]

$$I(q) \propto q^{\mathrm{Df}(3-\tau)} \quad (6)$$

The grain size obtained by a fractal interpretation equals $R = 1.5$ nm, which is lower than the value of $R = (4.37 \pm 0.72)$ nm obtained by the Guinier approximation. At the present we can only conclude that the fractal structure of V/Ce oxide with 55 atom % of V is preserved upon the intercalation of Li^+ ions. The detailed discussion on the fractal nature of this material, which is probably the reason for discrepancies between GISAXS and AFM data (Table 2) for this material, will be published elsewhere.

CONCLUSION

In conclusion, the present study showed that GISAXS and GIXR at the ELETTRA light source could be applied for grain size, specific surface and layer thickness determination in nanosized films of V_2O_5 and V/Ce oxides on a glass substrate as well as for following the process of the intercalation of Li^+ ions into the porous nanostructured films. The particular morphology obtained for samples prepared at 38 atom % and 55 atom % of V in V/Ce oxide is quite suitable for application in electrochromic devices, in an advanced electrochemical cell concept and efficient new solar cells. The results obtained with the GIXR and GISAXS analyses of data are complementary to build a model of the nanophased layers. The grain size distribution by GISAXS at different depths of the film compared to TEM reveals the complex inner-layered and nanostructured nature of the film.

ACKNOWLEDGMENT

The Ministry of Education, Science and Sport of the Republic of Croatia, under the contract number (0098026), is thanked for its support of this work, as is the Ministry of Sciences and Technology of the Republic of Slovenia, under the contract number (P-024512).

REFERENCES AND NOTES

(1) Lučič-Lavčević, M.; Dubček, P.; Milat, O.; Etlinger, B.; Turković, A.; Šokčević D.; Amenitsch, H. Nanostructure of sol−gel TiO_2 thin films on glass substrate measured by small angle scattering of synchrotron light. *Mater. Lett.* **1998**, *36*, 56−60.
(2) Turković, A.; Lučić-Lavčević, M.; Drašner, A.; Dubček, P.; Milat, O.; Etlinger, B.; Amenitsch, H.; Rappolt, M. Small-angle X-ray scattering studies of nanophase TiO_2 thin films. *Mater. Sci. Eng. B* **1998**, *54*, 174−181.
(3) Lučić-Lavčević, M.; Turković, A.; Dubček, P.; Milat, O.; Etlinger, B.; Šokčević, D.; Laggner, P.; Amenitsch, H. Grazing-icidence small-angle scattering of synchrotron radiation on nanosized TiO_2 thin films obtained by chemical vapour deposition and spray method. *Fizika A* **1998**, *7*−*3*, 119−132.
(4) Turković, A.; Dubček, P.; Crnjak Orel, Z.; Bernstorff, S. Small angle scattering of synchrotron radiation on nanosized CeO_2 and CeO_2−SnO_2 thin films obtained by sol−gel dipcoating method. *Nanostructured Mater.* **1999**, *11*, *No. 7*, 909−915.
(5) Turković, A.; Dubček, P.; Bernstorff, S. Grazing-incidence small-angle and wide-angle scattering of synchrotron radiation on nanosized CeO_2 thin films. *Mater. Sci. Eng. B* **1999**, *58*, 263−269.
(6) Turković, A.; Crnjak Orel, Z.; Dubček P.; Amenitsch, H. X-ray scattering measurements on nanosized TiO_2 micelles. *Solar Energy Mater. Solar Cells* **1999**, *59*, 387−392.
(7) Turković, A. Grazing-incidence SAXS/WAXD on nanosized TiO_2 films obtained by ALE. *Mater. Sci. Eng. B* **2000**, *75*, 85−91.
(8) Turković, A.; Crnjak Orel, Z.; Kosec, M. Electron microscopy studies of TiO_2 micelles. *Solar Energy Mater. Solar Cells* **2000**, *62*, 392−334.
(9) Turković, A.; Crnjak Orel, Z.; Dubček, P. Grazing-incidence small-angle X-ray scattering on nanosized vanadium oxide and V/Ce oxide films. *Mater. Sci. Eng. B* **2001**, *79/1*, 11−15.
(10) Posedel, D.; Turković, A.; Dubček P.; Crnjak Orel, Z. Grazing-incidence X-ray reflectivity on nanosized vanadium oxide and V/Ce oxide films, *Mater. Sci. Eng. B* **2002**, *90*, 154−162.
(11) Lučić-Lavčević, M.; Turković, A. The measurements of particle/crystallite size in nanostructured TiO_2 films by SAXS/WAXD method. *Scripta Mater.* **2002**, *46*, *Iss. 7*, 501−505.
(12) Lučić-Lavčević, M.; Turković, A. SAXS/WAXD on thermally annealed nanostructured TiO_2 fillms. *Thin Solid Films* **2002**, *419*, 105−113.
(13) Car, T.; Radić, N.; Turković, A. UV Photoconductivity of Nanophased TiO_2 Thin Films Annealed in Oxygen. *Jpn. J. Appl. Phys.* **2002**, *41*, 5618−5623.
(14) Crnjak Orel, Z.; Graberšček, M.; Turković, A. Electrical and spectroscopical characterisation of nanocrystalline V/Ce oxides. *Solar Energy Mater. Solar Cells* **2002**, in press.
(15) Turković, A.; Hrestak, K.; Dubček, P.; Crnjak Orel, Z. Small-angle X-ray scattering of synchrotron light source on nanostructured V/Ce oxide films. *Strojarstvo* **2002**, *3*−*6*, 211−217.
(16) Amenitsch, H.; Bernstorff, S.; Laggner, P. *Rev. Sci. Instrum.* **1995**, *66*, 1624.
(17) Amenitsch, H.; Rappolt, M.; Kriechbaum, M.; Mio, H.; Laggner, P.; Bernstorff, S. Small-Angle X-ray Scattering − Beamline at ELETTRA: A New Powerful Station for structural Investigations with Synchrotron Radiation, *Book of Abstracts*: Sixth Croatian-Slovenian Crystallographic Meeting, June 19−21, 1997, 56, Umag, Croatia.
(18) Dubček, P.; Milat, O.; Lučić-Lavčević, M.; Turković, A.; Etlinger, B.; Amenitsch, H. Small-Angle X-ray Scattering and X-ray reflection on Thin Films, *Book of Abstracts*: Sixth Croatian-Slovenian Crystallographic Meeting June 19−21, 1997, 57, Umag, Croatia.
(19) Guinier, A. *Ann. Phys., Paris* **1939**, *12*, 161.
(20) Porod, G. *Kolloid-Z. Z. Polym.* **1951**, *124*, 83.
(21) Porod, G. *Kolloid-Zeitschrift und Zeitschrift fur Polymere* **1952**, *125*, 108.
(22) Porod, G. *Kolloid-Z. Z. Polym.* **1953**, *133*, 51.
(23) Turković, A.; Ivanda, M.; Popović, S.; Tonejc, A. M.; Gotić, M.; Dubček, P.; Musić, S. *J. Mol. Struct.* **1997**, *410*−*411*, 271.
(24) Granquist, C. G. *Handbook of Inorganic Electrochromic Materials*; Elsevier: Amsterdam, 1995.
(25) Crnjak Orel, Z.; Mušević, I. *Nanostructured Mater.* **1999**, *12*, 399.
(26) Crnjak Orel, Z. *Solid State Ionics* **1999**, *116*, 105.
(27) Sinha, S. K.; Sirota, E. B.; Garoff, S. *Phys. Rev.* B **1988**, *38*, 2297.
(28) Hamley, I. W.; Pedersen, J. S. *J. Appl. Cryst*. **1994**, *27*, 29.
(29) Crnjak Orel, Z.; Kušćer, D.; Kosec, M.; Turković, A. submitted for publication.
(30) Crnjak Orel, Z.; Orel, B. *J. Mater. Sci.* **1995**, *30*, 2284.
(31) Turković, A.; Crnjak Orel, Z. *Solid State Ionics* **1996**, *89*, 255.
(32) Crnjak Orel, Z. *Appl. Spectrosc*. **1999**, *53*, 241.
(33) Martin, J. E.; Hurd, A. J. *J. Appl. Cryst.* **1987**, *20*, 61.

CI030419J